

Empirical scaling of the vortex glass line above 1 T for high- T_c superconductors of varying anisotropy

B. Lundqvist, A. Rydh, Yu. Eltsev, Ö. Rapp, and M. Andersson

Department of Solid State Physics, Royal Institute of Technology, SE-100 44 Stockholm, Sweden

(Received 12 March 1998)

The resistive transition into a glassy vortex state in oxygen-deficient $\text{YBa}_2\text{Cu}_3\text{O}_{7-\delta}$ twinned single crystals of varying anisotropy γ ($8.7 \leq \gamma \leq 35$) has been studied with an applied magnetic field along the crystallographic c axis. For $B \geq 1$ T, the glass line is well described by the empirical relation $B_g = B_0[(1 - T/T_c)/(T/T_c)]^\alpha$, where $\alpha \approx 1$ and $B_0 \approx 1.85\Phi_0/(\gamma d)^2$. The successful fit to this relation both below and above an alleged crossover in the solid vortex state has important consequences for the H - T phase diagram of high-temperature superconductors. [S0163-1829(98)51722-5]

The importance of thermal fluctuations, the extreme type-II character, and the large anisotropy of high-temperature superconductors give rise to a soft vortex system with a number of interesting features.¹ In particular, this results in a separation of the mixed state into a low-temperature vortex solid with a nonzero critical current density and a high-temperature vortex liquid with energy dissipation for all currents. In clean, optimally doped $\text{YBa}_2\text{Cu}_3\text{O}_{7-\delta}$ (YBCO) single crystals, a first-order transition has been observed and interpreted as a melting transition between a low-temperature Abrikosov lattice and a high-temperature vortex liquid.^{2,3} For disordered samples the vortex liquid freezes through a continuous second-order transition into a glassy state, whose properties depend on the kind of disorder.⁴⁻⁶ The boundary between the solid and liquid phases is strongly affected by the anisotropy of the material, with the vortex solid more suppressed for materials with higher anisotropy.^{7,8}

For magnetic fields $B \parallel c$ axis, a crossover between three-dimensional (3D) and two-dimensional (2D) vortex fluctuations has been proposed^{1,4} at a field $B_{2D} \approx \Phi_0/(\gamma d)^2$, where Φ_0 is the flux quantum, d the interplane spacing, and $\gamma = (m_c/m_{ab})^{1/2}$ is the anisotropy. Experimentally, various signs of a field-induced crossover have been observed in both clean and disordered materials.⁸⁻¹⁰ In oxygen-deficient thin films of YBCO, deviations from a power-law behavior $B_g \propto (1 - T/T_c)^{3/2}$ of the vortex glass line have been observed at an anisotropy-dependent field B^* and taken as evidence for reaching the 2D regime.¹¹

In this paper we study the influence of anisotropy on the vortex glass line using a test system consisting of oxygen-deficient single crystals of YBCO. By varying the oxygen content in the CuO_2 chains, the coupling between charge carriers in adjacent CuO_2 planes and thereby the anisotropy γ is changed.¹² By increasing the anisotropy, B^* can be lowered to experimentally accessible values in this system. We study the vortex glass line from the vortex liquid side, and find the disappearance of resistivity to be well described by $B_g = B_0[(1 - T/T_c)/(T/T_c)]^\alpha$ for magnetic fields below as well as above B^* with an exponent $\alpha \approx 1$. This suggests that the vortex dynamics remains essentially unchanged when increasing the field through B^* , indicating that the vortex system is 3D (or close to 3D) both below and above B^* . The

experimentally obtained field $B_0 \equiv B_g(T_c/2)$, which varies as $B_0 = 1.85\Phi_0/(\gamma d)^2$, is in good agreement with values of γ obtained from torque measurements.¹² Finally we successfully apply the proposed scaling relation to literature data on Y-, Bi-, and Tl-based thin films and discuss its implications for the H - T phase diagram of high-temperature superconductors (HTSC).

Single crystals of YBCO were grown by a self-flux method in yttria-stabilized zirconia crucibles as previously described.¹³ Twinned crystals of varying oxygen content were obtained by annealing for two weeks at various temperatures in air. Compared to YBCO powder, x-ray diffraction measurements showed a slightly larger c -axis lattice parameter, which increased continuously with decreasing T_c .

Electrical contacts were prepared by applying strips of silver paint, followed by heat treatment under the same conditions as during annealing, giving contact resistances below 1.5 Ω . Typical dimensions of the samples were $0.5 \times 0.2 \times 0.03$ mm³. Measurements of the in-plane resistance for magnetic fields $0 \leq B \leq 12$ T applied along the c axis were made with a current $I = 0.3$ mA and a voltage resolution down to 0.3 nV. The samples were cooled in a field through the superconducting transitions and data were recorded during increasing temperatures.

Figure 1 shows the in-plane resistance for one of our

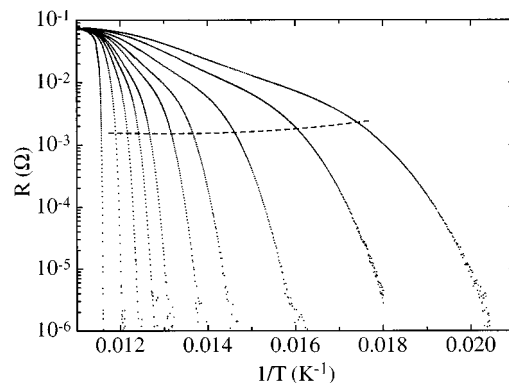


FIG. 1. Arrhenius plot of the resistive transitions for sample 2 in magnetic fields $B \parallel c$ axis of, from left to right, 0, 0.5, 1, 1.5, 2, 3, 4, 6, 9, and 12 T. The upper limit for the applicability of the Vogel-Fulcher relation $(d \ln R/dT)^{-1} \propto (T - T_g)$ is marked by the dashed line.

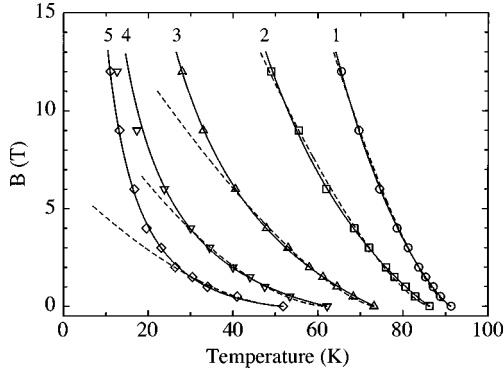


FIG. 2. Vortex glass transition lines determined from the disappearance of resistance for five YBCO samples of varying anisotropy. Solid lines are fits to $B_g = B_0[(1 - T/T_c)/(T/T_c)]^\alpha$ with T_c , B_0 , and α given in Table I. Dashed lines are described by $B_g \propto (1 - T/T_c)^n$, with $n \approx 1.4$. The latter description fails at high magnetic fields for the most anisotropic samples.

samples at magnetic fields $B \parallel c$ axis. A common feature of all samples is that the upper part of the transitions, $R > 0.05R_n$, follows a thermally activated behavior $R = R_0 \exp(-U/k_B T)$ as earlier observed.¹⁴ At lower temperatures a glassy regime is approached, characterized by a diverging activation energy and a truly zero resistance below a certain field-dependent temperature $T_g(B)$. The resistivity in this low-temperature region is still almost ohmic, and the determination of $T_g(B)$, to be described below, is not appreciably affected by the current level used in our experiment. For the optimally doped sample (sample 1), the crossover between the two temperature regimes is close to the temperature at which the first-order transition occurs in clean samples, which is significantly higher than our $T_g(B)$.¹⁵ According to the vortex glass model, the resistance at low currents goes to zero at the glass temperature T_g as $R \propto (T - T_g)^{\nu(z-1)}$, where ν and z are the static and dynamic critical exponents, respectively.⁴ Consequently $T_g(B)$ can be extracted by applying the Vogel-Fulcher relation $(d \ln R/dT)^{-1} \propto (T - T_g)$ to the resistive tails. Below the dashed line in the inset of Fig. 1, our data show good linear relations in agreement with this expression. In other studies this method for finding $T_g(B)$ has been shown to be consistent with a vortex glass scaling of the current-voltage (I - V) characteristics.¹¹ From the inverse of the slopes we find the scaling exponent $s = \nu(z-1)$ to fall in the range of 4 ± 1.5 for all samples and magnetic fields, which is somewhat smaller than previously observed for more disordered thin films.¹⁶

The magnetic field dependence of the measured glass transitions is shown in Fig. 2. The expression $B_g \propto (1 - T/T_c)^n$, which has frequently been used^{11,17} to describe the vortex glass line below B^* is shown by dashed lines in Fig. 2. We obtain an exponent $n = 1.4 \pm 0.1$ for all samples except for samples 4 and 5 which have $n \approx 1.7$. It is clearly seen that the fit breaks down for the most anisotropic samples, demonstrating that B^* has been decreased to experimentally accessible values by increasing the anisotropy.

We find, however, that an empirical equation better describes the temperature dependence of the vortex glass line, including fields both below and above B^* ;

TABLE I. Properties of $\text{YBa}_2\text{Cu}_3\text{O}_{7-\delta}$ single crystals. For consistency T_c is taken as the temperature for the onset of resistivity (resolution limit of our experiment) in zero magnetic field. B_0 and α were obtained by fitting Eq. (1) to the vortex glass lines. γ was estimated from $B_0 = C\phi_0/(\gamma d)^2$.

Sample	T_c (K)	Annealing	B_0 (T)	α	γ
1	91.3	O ₂ , 450 °C	36.9	1.21	8.7
2	86.2	air, 500 °C	16.2	1.05	13
3	73.2	air, 525 °C	7.47	0.98	19
4	62.2	air, 600 °C	3.69	1.06	28
5	51.8	air, 700 °C	2.27	1.27	35

$$B_g = B_0[(1 - T/T_c)/(T/T_c)]^\alpha. \quad (1)$$

A comparison between the two functional forms of B_g shows that they are similar only for temperatures down to $T_c/2$. This explains the observation that deviations from $B_g \propto (1 - T/T_c)^n$ seem to set in at $T \approx 0.5T_c$.^{11,17} Note that Eq. (1) implies that the characteristic magnetic field $B_0 \equiv B_g(T_c/2)$, and therefore $B_0 \approx B^*$. The solid curves in Fig. 2 were calculated from Eq. (1) with the values of B_0 , T_c , and α given in Table I. An excellent description of data is obtained by this form. Small uncertainties below 1 T can possibly be attributed to a nonuniform vortex distribution at low fields. For sample 4, there is some discrepancy above 6 T. We suggest that these discrepancies may be connected with sample inhomogeneities as reflected in a larger zero-field transition width ($\Delta T_c \approx 6$ K) and a small c -axis contribution as observed in the normal-state resistivity of this sample.

From Table I and Fig. 2 we see that the fitted B_0 roughly agrees with the field B^* , at which the $(1 - T/T_c)^n$ power law breaks down for samples 3–5 with accessible B^* . We therefore write $B_0 = C\Phi_0/(\gamma d)^2$ as previously made for B^* .¹¹ If we take d as the c -axis lattice parameter $d = 11.7$ Å, the constant C can be determined by using our fitted B_0 and a value of γ obtained from torque measurements by Chien *et al.*¹² In order to have a strict one-to-one correspondence between γ and T_c , we make this comparison for sample 3, which has a T_c in between the 60 K and 90 K plateaus of YBCO. The obtained value, $C = 1.85$, is then used to calculate the anisotropy of the other four samples. Good agree-

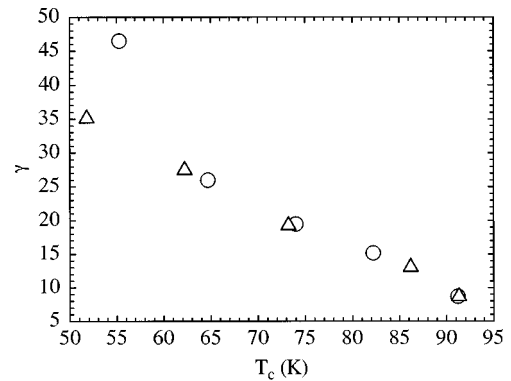


FIG. 3. Anisotropy γ versus T_c for oxygen-deficient single crystals of YBCO. The values in this study (Δ) were obtained by assuming $B_0 = C\phi_0/(\gamma d)^2$ and are in good agreement with results from torque magnetometry (see Ref. 12) (\circ), except for the most anisotropic sample as discussed in the text.

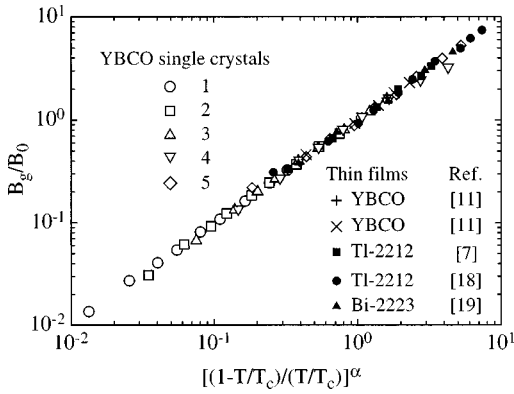


FIG. 4. Scaling of the vortex glass line according to Eq. (1). Shown are data from single crystals of YBCO (present work), thin films of deoxygenated YBCO (Ref. 11, +: $T_c=57$ K, \times : $T_c=48.5$ K), thin films of Tl-2212 (Refs. 7 and 18), and a thin film of Bi-2223 (Ref. 19). T_c , B_0 , and α are shown in Table I for the single crystals and in Table II for the thin films.

ment for samples 1–4, between our analysis of γ from the fitted B_0 and the values of Ref. 12, is shown in Fig. 3, giving strong evidence for the proposed anisotropy dependence of B_0 . However, we do not observe the strong increase of γ below the 60 K plateau, as seen in Ref. 12. As noted by these authors, their lower annealing temperatures should result in an oxygen distribution with more local ordering, and consequently a higher critical temperature in this region.

The applicability of Eq. (1) was further investigated with data from the literature for different superconducting thin films. B_0 was evaluated as $B_g(T_c/2)$ and B_g/B_0 was calculated as a function of $[(1-T/T_c)/(T/T_c)]^\alpha$, with α as the only adjustable parameter. Data for oxygen-deficient YBCO thin films¹¹ with $T_c=57$ K and 48.5 K, as well as for the more anisotropic Tl-2212^{7,18} and Bi-2223¹⁹ superconductors, are shown in Fig. 4 together with our data from Fig. 2. The parameters B_0 and α for the thin-film superconductors are given in Table II. The results illustrate that Eq. (1) can be used over at least three orders of magnitude in B_g/B_0 . The exponent α depends on the material with values around 1 for YBCO and in the range of 1.6–1.8 for the Bi and Tl thin films.

We now consider possible theoretical support for Eq. (1). In the absence of disorder, the vortex solid-to-liquid transition is a melting transition, which can be derived from a Lindemann criterion $\langle u^2 \rangle_{\text{th}} = c_L^2 a_0^2$, where c_L is the Lindemann number ($0.1 < c_L < 0.3$) and a_0 is the vortex lattice constant.²⁰ Close to T_c this gives a temperature dependence $B \propto [(1-T/T_c)/(T/T_c)]^2$, which is sometimes simplified to a $(1-T/T_c)^2$ power law.²¹ Blatter and Ivlev included the effect of quantum fluctuations $\langle u^2 \rangle_q$ on the melting phenomenon.²² The temperature dependence then becomes more complicated and no closed form for the field dependence of the melting line can be obtained. Qualitatively, however, the effect of quantum fluctuations is a shift of the melting line towards lower fields, corresponding to a value of α smaller than 2. In both these theories the prefactor approximately varies as $1/\gamma^2$. Thus, the proposed temperature and anisotropy dependence of the vortex glass behavior in our samples does not seem unreasonable.

TABLE II. Critical temperature T_c and parameters B_0 and α according to Eq. (1) for various thin film samples: Deoxygenated YBCO (magnetic field range $B=1-5$ T), Tl-2212 ($B=0.5-5$ T in Ref. 7 and 0.5–12 T in Ref. 18), and Bi-2223 ($B=0.5-6$ T).

Sample	T_c (K)	B_0 (T)	α	Ref.
YBCO	57.0	3.07	0.95	11
YBCO	48.5	2.17	1.12	11
Tl-2212	100	1.50	1.59	7
Tl-2212	102.5	1.61	1.82	18
Bi-2223	96	1.31	1.82	19

The description of $B_g(T)$, illustrated in Fig. 2, is remarkably simple and accurate. The fact that one functional form describes the experimental data on both sides of B^* suggests that the beginning of deviations from $B_g \propto (1-T/T_c)^n$ ($n \sim 3/2$) at B^* should not be associated with a dimensional crossover field B_{2D} . It also indicates that the same physical mechanism is responsible for the disappearance of resistance in both magnetic field regimes in the liquid state. Furthermore, the good fits presented here are correlated to half the transition temperature through $B_0 \equiv B_g(T_c/2)$. This significance of a certain temperature is not expected for a behavior that is field induced, as the crossover field B_{2D} . We also find no changes in vortex glass behavior or in critical exponents around B^* as one may expect at a dimensional crossover, since the scaling exponents depend on dimensionality. This is also consistent with constant critical exponents on both sides of B^* as obtained from a vortex glass scaling of the I - V characteristics.¹¹ We therefore conclude that the vortex system is 3D (or close to 3D) both below and above B^* in the vortex liquid.

The present results have important consequences for the vortex solid phase. Signs of a crossover in the vortex solid have been observed both in clean^{8,23} and disordered^{9,10} samples. The absence of any signs of a crossover in the vortex liquid and the smooth shape of the glass line in our disordered samples therefore suggest that a possible crossover can neither continue above, nor end on the glass line in a tricritical point. The phase diagram therefore differs from the one obtained for clean samples. One possibility is that the crossover becomes suppressed when approaching the glass line, as was observed in Ref. 10.

In summary, we have studied the temperature dependence of the vortex glass line for oxygen-deficient $\text{YBa}_2\text{Cu}_3\text{O}_{7-\delta}$ single crystals of varying anisotropy. The semiempirical relation $B_g = B_0 [(1-T/T_c)/(T/T_c)]^\alpha$, with $B_0 = 1.85\Phi_0/(\gamma d)^2$, was found to well describe the temperature dependence of the glass transition both below and above the purported crossover field B^* . The above relation was also successfully applied to the vortex glass lines for thin films including the more anisotropic Tl-2212 and Bi-2223 superconductors.

Financial support from the Swedish Natural Science Research Council, the Swedish Research Council for Engineering Sciences, the Göran Gustafsson Foundation, and the Swedish Superconductivity Consortium is gratefully acknowledged.

- ¹G. Blatter, M. V. Feigel'man, V. B. Geshkenbein, A. I. Larkin, and V. M. Vinokur, *Rev. Mod. Phys.* **66**, 1125 (1994).
- ²A. Schilling, R. A. Fisher, N. E. Phillips, U. Welp, D. Dasgupta, W. K. Kwok, and G. W. Crabtree, *Nature (London)* **382**, 791 (1996).
- ³U. Welp, J. A. Fendrich, W. K. Kwok, G. W. Crabtree, and B. W. Veal, *Phys. Rev. Lett.* **76**, 4809 (1996).
- ⁴D. S. Fisher, M. P. A. Fisher, and D. A. Huse, *Phys. Rev. B* **43**, 130 (1991).
- ⁵T. Giamarchi and P. Le Doussal, *Phys. Rev. B* **52**, 1242 (1995); **55**, 6577 (1997).
- ⁶D. R. Nelson and V. M. Vinokur, *Phys. Rev. B* **48**, 13 060 (1993).
- ⁷J. Deak, M. McElfresh, D. W. Face, and W. L. Holstein, *Phys. Rev. B* **52**, R3880 (1995).
- ⁸R. Cubitt, E. M. Forgan, G. Yang, S. L. Lee, D. McK. Paul, H. A. Mook, M. Yethiraj, P. H. Kes, T. W. Li, A. A. Menovsky, Z. Tarnawski, and K. Mortensen, *Nature (London)* **365**, 407 (1993).
- ⁹H. Obara, M. Andersson, L. Fàbrega, P. Fivat, J.-M. Triscone, M. Decroux, and Ø. Fischer, *Phys. Rev. Lett.* **74**, 3041 (1995).
- ¹⁰H. H. Wen, A. F. Th. Hoekstra, R. Griessen, S. L. Yan, L. Fang, and M. S. Si, *Phys. Rev. Lett.* **79**, 1559 (1997).
- ¹¹Lifang Hou, J. Deak, P. Metcalf, M. McElfresh, and G. Preosti, *Phys. Rev. B* **55**, 11 806 (1997).
- ¹²T. R. Chien, W. R. Datars, B. W. Veal, A. P. Paulikas, P. Kostic, Chun Gu, and Y. Jiang, *Physica C* **229**, 273 (1994).
- ¹³Yu. Eltsev, W. Holm, and Ö. Rapp, *Phys. Rev. B* **49**, 12 333 (1994).
- ¹⁴T. T. M. Palstra, B. Batlogg, R. B. van Dover, L. F. Schneemeyer, and J. V. Waszczak, *Phys. Rev. B* **41**, 6621 (1990).
- ¹⁵B. Lundqvist, A. Rydh, Ö. Rapp, and M. Andersson, *Physica C* **282-287**, 1959 (1997).
- ¹⁶R. H. Koch, V. Foglietti, W. J. Gallagher, G. Koren, A. Gupta, and M. P. A. Fisher, *Phys. Rev. Lett.* **63**, 1511 (1989).
- ¹⁷C. C. Almasan, M. C. de Andrade, Y. Dalichaouch, J. J. Neumeier, C. L. Seaman, M. B. Maple, R. P. Guertin, M. V. Kuric, and J. C. Garland, *Phys. Rev. Lett.* **69**, 3812 (1992).
- ¹⁸B. Lundqvist, J. Larsson, A. Herting, Ö. Rapp, M. Andersson, Z. G. Ivanov, and L.-G. Johansson (unpublished).
- ¹⁹P. Wagner, U. Frey, F. Hillmer, and H. Adrian, *Phys. Rev. B* **51**, 1206 (1995).
- ²⁰A. Houghton, R. A. Pelcovits, and A. Sudbø, *Phys. Rev. B* **40**, 6763 (1989).
- ²¹W. K. Kwok, S. Fleshler, U. Welp, V. M. Vinokur, J. Downey, G. W. Crabtree, and M. M. Miller, *Phys. Rev. Lett.* **69**, 3370 (1992).
- ²²G. Blatter and B. I. Ivlev, *Phys. Rev. B* **50**, 10 272 (1994).
- ²³M. F. Goffman, J. A. Herbsommer, F. de la Cruz, T. W. Li, and P. H. Kes, *Phys. Rev. B* **57**, 3663 (1998).